UNIVERSIDAD REGIONAL AMAZÓNICA IKIAM

FACULTAD DE CIENCIAS DE VIDA

CARRERA DE BIOTECNOLOGÍA

EFFECT OF CALCINATION TIME ON THE PHOTOCATALYTIC ACTIVITY OF BiOI MICROSPHERES TO DEGRADE IBUPROFEN UNDER VISIBLE LIGHT.

Proyecto de investigación previo a la obtención del Título de:

INGENIERA EN BIOTECNOLOGÍA

AUTOR: MARIA JOSÉ AUQUILLA VILLAMAGUA

TUTOR: Mgs. LUIS MIGUEL QUISHPE QUISHPE

CO-TUTOR: Ph.D MIGUEL HERRERA ROBLEDO

Tena – Ecuador

2024

Carrera de Biotecnología

Declaración de derecho de autor, autenticidad y responsabilidad

Tena, 3 de septiembre del 2024

Yo, Maria José Auquilla Villamagua, con documento de identidad 1105790867, declaro que los resultados obtenidos en la investigación que presento en este documento final, previo a la obtención del título de Ingeniería en Biotecnología, son absolutamente inéditos, originales, auténticos y personales.

En virtud de lo cual, el contenido, criterios, opiniones, resultados, análisis, interpretaciones, conclusiones, recomendaciones y todos los demás aspectos vertidos en el presente documento, son de mi autoría y de mi absoluta responsabilidad.

MARIA JOSE AUQUILLA VILLAMAGUA

Firmado digitalmente por MARIA JOSE AUQUILLA VILLAMAGUA
Fecha: 2024.09.03 12:21:01 -05'00'

Maria José Auquilla Villamagua

CI: 1105790867

Carrera de Biotecnología

Autorización de publicación en el repositorio institucional

Tena, 3 de septiembre del 2024

Yo, Maria José Auquilla Villamagua, con documento de identidad 1105790867 en calidad de autor/a y titular de los derechos morales y patrimoniales del trabajo de titulación "Effect of calcination time on the photocatalytic activity of BiOI microspheres to degrade ibuprofen under visible light", de conformidad con el Art. 114 del CÓDIGO ORGÁNICO DE LA ECONOMÍA SOCIAL DE LOS CONOCIMIENTOS, CREATIVIDAD E INNOVACIÓN, reconozco a favor de la Universidad Regional Amazónica Ikiam una licencia gratuita, intransferible y no exclusiva para el uso no comercial de la obra, con fines estrictamente académicos.

Así mismo autorizo a la Universidad Regional Amazónica Ikiam para que realice la publicación de este trabajo de titulación en el Repositorio Institucional de conformidad a lo dispuesto en el Art. 144 de la Ley Orgánica de Educación Superior.

Atentamente,

MARIA JOSE AUQUILLA VILLAMAGUA

Firmado digitalmente por MARIA JOSE AUQUILLA VILLAMAGUA
Fecha: 2024.09.03 12:21:34 -05'00'

Maria José Auquilla Villamagua

CI: 1105790867

Carrera de Biotecnología

Certificado de dirección de trabajo de titulación

Tena, 3 de septiembre del 2024

Certifico que el trabajo de titulación: “Effect of calcination time on the photocatalytic activity of BiOI microspheres to degrade ibuprofen under visible light”, aprobado bajo el mecanismo de titulación de: artículo, fue realizado por Maria José Auquilla Villamagua, bajo mi dirección.

El mismo ha sido revisado en su totalidad y analizado por la herramienta de verificación de similitud de contenido; por lo tanto, cumple con los requisitos teóricos, científicos, técnicos, metodológicos y legales establecidos por la Universidad Regional Amazónica Ikiam, para su entrega y defensa.

Firmado electrónicamente por:
LUIS MIGUEL QUISHPE QUISHPE

Luis Miguel Quishpe Quishpe

C.I: 1500843048

Tutor

Firmado electrónicamente por:
MIGUEL HERRERA ROBLEDO

Miguel Herrera Robledo

C.I: 1550516452

Cotutor

AGRADECIMIENTOS

Quiero expresar mi más profundo agradecimiento a la Universidad Regional Amazónica Ikiam por brindarme la oportunidad de formarme como profesional y por ser mi guía en esta apasionante carrera.

Asimismo, extiendo mi gratitud a mis mentores Miguel Quishpe, Miguel Herrera y Michael Zuarez. Su convicción de que el conocimiento científico debe compartirse y nutrirse a través del diálogo y la colaboración ha sido una inspiración constante. Sus enseñanzas no solo han fortalecido mi comprensión de la ciencia, sino que también me han inspirado a buscar maneras de contribuir positivamente a nuestra sociedad.

De manera especial, quiero agradecer a Andrea Salgado y Carolina Ñacato por su apoyo continuo y guía inestimable. Su compromiso constante ha enriquecido mi experiencia académica y consolidado mi confianza en el camino que he elegido.

A mis amigos, tanto a los que están a mi lado como a los que ya no están, gracias por llenar mi vida de momentos inolvidables y por enseñarme lecciones que perdurarán para siempre. Su amistad ha sido una fuente constante de alegría y sabiduría, y sus recuerdos vivirán eternamente en mi corazón.

A Leonardo, por ser mi constante fuente de amor, paciencia y apoyo incondicional, fueron fundamentales para mantenerme enfocada y motivada.

Finalmente, a mi familia, que ha estado presente pese a la distancia. Gracias por creer en mí, por apoyarme en cada paso del camino y por comprender la importancia de esta experiencia para mi desarrollo personal y profesional. Su amor y apoyo han sido fundamentales para alcanzar mis metas.

DEDICATORIA

A mis padres y familia, quienes han sido mis faros de sabiduría y amor.

A ti, mi compañero de café y de vida, gracias por ser mi constante apoyo y fuente de inspiración

TABLA DE CONTENIDO

CARATULA

DECLARACIÓN DE DERECHO DE AUTOR, AUTENTICIDAD Y RESPONSABILIDAD II

AUTORIZACIÓN DE PUBLICACIÓN EN EL REPOSITORIO INSTITUCIONAL III

CERTIFICADO DE DIRECCIÓN DE TRABAJO DE TITULACIÓN IV

AGRADECIMIENTOS V

DEDICATORIA VI

ÍNDICE DE TABLAS VIII

ÍNDICE DE FIGURAS IX

RESUMEN X

ABSTRACT XI

GRAPHICAL ABSTRACT XII

INTRODUCTION 2

METHODOLOGY 4

2.1. MATERIALS AND REAGENTS 4

2.2. SYNTHESIS OF $BI_XO_YI_Z$ FLOWER-LIKE MICROSPHERES 4

2.3. STRUCTURAL, MORPHOLOGICAL AND CHEMICAL CHARACTERIZATION 5

2.4. PHOTOCATALYTIC DEGRADATION OF IBUPROFEN 5

RESULTS AND DISCUSSION 7

CONCLUSIONS 17

FUNDING SOURCES 17

AUTHOR CONTRIBUTIONS: CREDIT 18

ACKNOWLEDGMENT 18

REFERENCES

ÍNDICE DE TABLAS

Table 1: Experimental Design for Evaluating Photocatalytic Degradation of Ibuprofen Using Calcined Materials.....6

Table 2. Evolution of the morphology of nanostructured flower-like microspheres: Diameter and thickness of $Bi_xO_yI_z$ as a function of time (0, 15, 30, 45 and 60 min) of calcination. 11

ÍNDICE DE FIGURAS

Figure. 1 XRD patterns of BiOI samples calcinated at different times: a) Bi-0, b) Bi-15, c) Bi-30, d) Bi-45, and e) Bi-60. 9

Figure. 2 SEM images of the samples synthesized at different calcination times Bi-0 (a-b), Bi-15 (c-d), Bi-30 (e-f), Bi-45 (g-h) and Bi-60 (i-j). 11

Figure. 3 Elemental analysis performed by EDS of samples synthesized and calcined at different times: (a) Bi-0, (b) Bi-15, (c) Bi-30, (d) Bi-45, and (e) Bi-60. 13

Figure. 4 UV–vis absorption spectra of samples: (a) 3 ppm ibuprofen (b) photolysis test of 3 ppm ibuprofen and photocatalytic degradation of ibuprofen using (c)B-0, (d) B-15, (e) B-30, (f) B-45, and (g) B-60. 15

Figure. 5. Analysis of the absorbance at 262 nm for samples B-0, B-15, B-30, B-45 and B-60. 16

RESUMEN

El ibuprofeno, un fármaco antiinflamatorio no esteroideo ampliamente utilizado, se ha convertido en una preocupación medioambiental emergente debido a su presencia en diversas fuentes de agua, incluidas las aguas superficiales, las aguas subterráneas e incluso el agua potable. Esta contaminación plantea riesgos potenciales tanto para la salud humana como para el medio ambiente, por lo que es necesario desarrollar métodos eficientes y sostenibles para eliminar el ibuprofeno de los cuerpos de agua. Este estudio investiga la síntesis de BiOI mediante un método solvotermal y examina el impacto del tiempo de calcinación (0, 15, 30, 45 y 60 minutos) a 410 °C sobre su morfología, composición química y actividad fotocatalítica. Los resultados indican que el aumento del tiempo de calcinación mejora la cristalinidad e induce transformaciones cristalinas, dando lugar a la formación de fases BiOI y $Bi_4O_5I_2$ así como heterouniones BiOI/ $Bi_4O_5I_2$ y $Bi_4O_5I_2$/ Bi_5O_7I. Las muestras B-30, B-45 y B-60 exhibieron actividad fotocatalítica, confirmada por la aparición de una banda de absorbancia a 262 nm, característica de los productos intermedios de la degradación del ibuprofeno en agua. Sin embargo, la muestra B-30 presentó la mayor eficiencia en la degradación del ibuprofeno y sus intermediarios. Estos hallazgos resaltan el potencial de los materiales basados en BiOI para la eliminación efectiva del ibuprofeno en aguas contaminadas.

Palabras clave: BiOI, Calcinación, Heterouniones, Ibuprofeno, Transformación de fase, Fotocatálisis, Luz visible.

ABSTRACT

Ibuprofen, a widely used non-steroidal anti-inflammatory drug, has become an emerging environmental concern due to its presence in various water sources, including surface water, groundwater and even drinking water. This contamination poses potential risks to both human health and the environment, necessitating the development of efficient and sustainable methods to remove ibuprofen from water bodies. This study investigates the synthesis of BiOI by a solvothermal method and examines the impact of calcination time (0, 15, 30, 45 and 60 min) at 410 °C on its morphology, chemical composition and photocatalytic activity. The results indicate that increasing the calcination time enhances the crystallinity and induces crystalline transformations, leading to the formation of BiOI and $Bi_4O_5I_2$ phases as well as BiOI/ $Bi_4O_5I_2$, and $Bi_4O_5I_2$/ Bi_5O_7I heterojunctions. Samples B-30, B-45 and B-60 exhibited photocatalytic activity, confirmed by the appearance of an absorbance band at 262 nm, characteristic of the intermediate products of ibuprofen degradation in water. However, sample B-30 presented the highest efficiency in the degradation of ibuprofen and its intermediates. These findings highlight the potential of BiOI-based materials for the effective removal of ibuprofen in contaminated water.

Keywords: BiOI, Calcination, Heterojunctions, Ibuprofen, Phase transformation, Photocatalysis, Visible light.

GRAPHICAL ABSTRACT

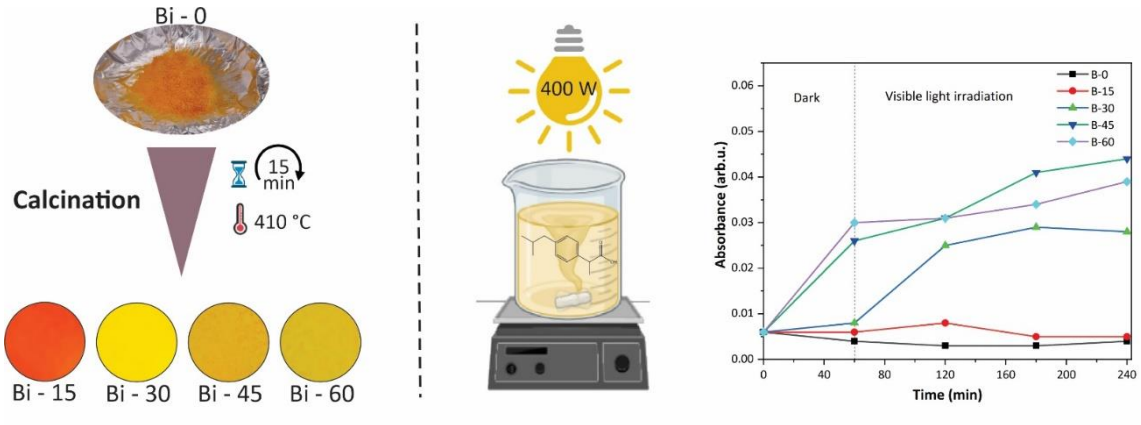

Environmental Research

Link: https://www.sciencedirect.com/journal/environmental-research/publish/guide-for-authors

Effect of calcination time on the photocatalytic activity of BiOI microspheres to degrade ibuprofen under visible light.

Maria Auquilla-Villamagua[a].

[a]Universidad Regional Amazónica Ikiam, Muyuna Road km 7, San Juan de Tena, Napo, Ecuador.

1. INTRODUCTION

Currently, various pharmaceutical products have generated concern due to their persistence in water bodies [1]. Among them, ibuprofen has stood out due to is a nonsteroidal anti-inflammatory drug (NSAID) with one of the highest consumption demands, being included in the World Health Organization's "List of Essential Medicines" [2–4]. Thus, the excessive use of ibuprofen and the improper management of its residues has led to its detection in surface water, groundwater, drinking water, domestic water, and wastewater, with concentrations of 0.4 μg L−1 [5], 3.5 ng/L [6], 1.3 μg L−1 [5], 0.22 μg/L, and 8600 ng/L [6–8], respectively. These represents a high risk to the public health, since ibuprofen and its by-products can persist in aquatic environments, causing bioaccumulation and cytotoxic and genotoxic damage to living organisms, thereby affecting their development and reproduction [1,2,5,6]. In this regard, it is necessary to develop safe and efficient methods to remove ibuprofen in water bodies.

Among the water treatment methods developed, semiconductor photocatalysis has stood out for its high efficiency, low energy consumption, and operating cost [9]. Semiconductors based on bismuth oxyhalides, BiOX (X = Cl, Br, I), have attracted attention for their excellent optical and electronic characteristics [10–12]. Among them, bismuth oxyiodide (BiOI) [13,14] has been widely used for its narrow bandgap (i.e., 1.7-2.0 eV), which allows it to absorb photons of the visible light spectrum [27–3]. Thus, BiOI micro/nanostructures with various morphologies, such as flower-shaped microspheres, hollow microspheres, porous microspheres, ultrathin nanolayers, and solid spheres have been used for the degradation of dyes [20–22], bacteria [21], analgesics [13], antibiotics [15,23,24], and endocrine disruptors [25,26]. However, the photocatalytic performance of pure BiOI is limited by its high recombination rate of photogenerated charge carriers [15,20] and inadequate redox potentials to produce reactive oxygen species (ROS) [16,27,28]. Given this, several strategies have been developed to improve its performance, such as the calcination method [10,29,30].

The calcination method has improved the physicochemical, structural, and optical properties of semiconductor materials [29,31–33]. For example, Putri et al. [34] reported that calcination of BiOI between 100 °C and 550 °C generated a loss of iodine and the formation of materials richer in oxygen and bismuth, which in turn caused changes in their crystalline phase, crystallite size, morphology, surface area, and porous structure.

Moreover, this improved the redox potentials of the material by inducing changes in the top and bottom position of the valence and conduction bands, respectively. In this sense, several researchers have dedicated to evaluate the effect of calcination temperature on the BiOI properties to obtain bismuth-rich bismuth oxyiodides ($Bi_xO_yI_z$). For example, Guan et al. [19] and Huang et al [35] demonstrated that BiOI calcined at 410 °C showed greater photocatalytic activity compared to BiOI calcined at 100 [30], 350, and 380 [35], and 500 °C [10,34,35]. This is because calcination at 410°C promoted the formation of a heterojunction of two $Bi_xO_yI_z$ crystalline phases, thus inhibiting the recombination of photogenerated electrons and holes. Nevertheless, these investigations have not addressed the calcination time which can significantly influence the properties of the material [10]. Varying calcination time can lead to better control of transitions between crystalline phases, which in turn can lead to semiconductors with higher photocatalytic performance [10,34,35].

Therefore, this work aims: 1) to prepare $Bi_xO_yI_z$ photocatalysts using different calcination times of BiOI microspheres previously obtained by a solvothermal method. 2) To examines the physicochemical properties of the obtained $Bi_xO_yI_z$ photocatalysts using X-ray diffraction (XRD), scanning electron microscopy (SEM), and energy-dispersive X-ray spectroscopy (EDS), and 3) qualitative analysis between the calcination time of BiOI microspheres and the degradation rate of ibuprofen.

2. METHODOLOGY

2.1. Materials and reagents

Bismuth nitrate pentahydrate ($Bi(NO_3)_3 \cdot 5H_2O$, Sigma-Aldrich, ≥98%), potassium iodide (KI, ExiPlus, Multi-Compendial, 99.8%), ethylene glycol ($C_2H_4(OH)_2$, Sigma-Aldrich, ≥99%) were utilized for photocatalyst preparation without further purification. α-methyl-4-(isobutyl)phenylacetic acid, (±)-2-(4-isobutylphenyl)propanoic acid (ibuprofen, Sigma-Aldrich, Pharmaceutical Secondary Standard) was used as model contaminant.

2.2. Synthesis of $Bi_xO_yI_z$ flower-like microspheres

BiOI microspheres were synthesized by modifying the solvothermal method described by Zuarez-Chamba et al [25], adjusting the reaction temperature and time. Briefly, solution A was prepared by dissolving 3 mmol of ($Bi(NO_3)_3 * 5H_2O$) in 30 mL of ethylene glycol. The mixture was sonicated for 30 minutes, followed by continuous stirring at 500 rpm for an additional 30 minutes. Concurrently, solution B was prepared by dissolving 3 mmol of KI in 30 mL of ethylene glycol under continuous stirring (500 rpm). Solution B was then added dropwise (1 mL/min) to solution A under constant stirring (500 rpm).

After 30 minutes of stirring, the mixture was transferred to a 100 mL Teflon-lined stainless steel autoclave and incubated in an oven at 160 °C for 3 hours. Following the reaction, the mixture was filtered using a vacuum filtration system and washed sequentially with ultrapure water, 96% ethanol, and ultrapure water again. The obtained BiOI microspheres were dried in an oven at 60 °C for 4 hours.

Bismuth-rich bismuth oxyiodide (BixOyIz) samples were obtained by calcining the synthesized BiOI powder. 400 mg of BiOI powder was evenly distributed in a porcelain crucible and calcined in a muffle furnace (Thermo Scientific 48000) at 410 °C [19,35] for

varying durations: 0, 15, 30, 45, and 60 minutes. The resulting samples were labeled as Bi-0, Bi-15, Bi-30, Bi-45, and Bi-60, respectively.

2.3. Structural, morphological and chemical characterization

The crystalline structure of $Bi_xO_yI_z$ microspheres was characterized by X-ray diffraction (XRD) using a Malvern Panalytical Empyrean diffractometer equipped with a copper X-ray tube (Kα radiation, λ = 1.54056 Å). XRD data were collected in the 2θ range from 5° to 90° with a scanning step of 0.017°, at 45 kV and 40 mA. The morphology was observed by scanning electron microscopy (SEM) on a Tescan Mira 3 scanning electron microscope. SEM images and Image J software were used to determine the diameter of the $Bi_xO_yI_z$ microspheres. The elemental chemical composition of the powder microspheres was determined by X-ray energy dispersive spectroscopy (EDS) using a Bruker X-Flash 6-30 detector coupled to the SEM equipment, with a resolution of 123 eV at Mn Kα. Furthermore, to study more about $Bi_xO_yI_z$ crystal properties, the average crystal size value of annealed Bi-0, Bi-15, Bi-30, Bi-45, and Bi-60 was calculated using the Debye–Scherrer equation (1) [36–38]:

$$L = \frac{K\lambda}{\beta Cos\theta} \quad (1)$$

Where L represents the crystallite size, K (0.9) is a constant, λ (0.154 nm) is the wavelength of X-rays, β is the FWHM (full width at half maximum; in radian), and θ is the Bragg angle.

2.4. Photocatalytic degradation of ibuprofen

The photocatalytic activity of the calcined samples (B-0, B-15, B-30, B-45, and B-60) was evaluated by photocatalytic degradation of ibuprofen (3 ppm) in a photoreactor equipped with a white LED lamp (400 W, 6500 K), ventilation system and constant stirring (300 rpm).

Briefly, 100 mg of each sample was mixed with 350 ml of ibuprofen solution and sonicated for 10 min. After a dark adsorption period (60 min), the solution was irradiated for 180 min. 13mL aliquots were taken every 60 min during the dark and irradiation phases, and subsequently centrifuged at 4000 rpm at 4°C for 1 h. Then, a absorbance spectral scan of the ibuprofen in each aliquot was performed in the range from 190 to 300 nm to identify its maximum absorption band. This was performed in a UV-Vis-NIR spectrophotometer (Shimadzu). A calibration curve was then prepared with ibuprofen standard solutions (0-10 ppm) at the maximum peak of the absorbance band at 222 nm for quantification of the initial concentration. In addition, a photolysis experiment was performed under the same experimental conditions, but without photocatalyst, to determine the degradation of ibuprofen by photons of the light source used in this work.

The reaction conditions (i.e., photocatalyst dosage, initial ibuprofen concentration, reaction temperature, dark and visible light conditions) for all experiments were kept constant and each was performed in triplicate to ensure reproducibility. A detailed scheme of the experimental design is presented in Table 1.

Table 1: Experimental Design for Evaluating Photocatalytic Degradation of Ibuprofen Using Calcined Materials. X = condition to use for each sample. Na = not applicable

Sample	Calcination time (min)	Dark (60 min)	Visible light (180 min)	Initial Ibuprofen Concentration (3 ppm)	Photocatalyst dosage (0.2857 mg/mL)	Final Ibuprofen Concentration (mg/L)
B-0	0	x	x	x	x	Evaluate
B-15	15	X	X	X	X	Evaluate
B-30	30	X	X	X	X	Evaluate
B-45	45	X	X	X	X	Evaluate
B-60	60	X	X	X	X	Evaluate
Photolysis (control)	Na	X	X	X	Na	Evaluate

3. RESULTS AND DISCUSSION

3.1. Instrumental analysis of powdery BiOI microspheres

3.1.1. XRD

The crystalline phase of the calcinated samples was studied by X-ray diffraction (XRD). **Fig.1** shows the XRD patterns of Bi-0, Bi-15, Bi-30, Bi-45, and Bi-60 samples. For Bi-0, the diffraction peaks placed at 2θ: 8.513°, 24,45°, 28.935°, 31.754°, 32.752°, 35.251°, 36.26° 45.498°, 49.321°, 54.843°, 58.726°, 62.093°, 66.309°, 73.721, 75.321°, and 55.568 can be assigned to the (0 0 1), (0 1 1), (0 1 2), (1 1 0), (1 1 1), (0 1 3), (1 1 2), (0 2 0), (0 2 2), (1 2 2) , (1 1 5), (0 2 4), (2 2 0), (0 3 2), (1 3 0) and (1 3 4) crystalline planes of the tetragonal BiOI phase (ICDD #98-039-1354). These results are the same as the reported for BiOI microspheres [25]. After being calcinated for 15 min (B-15), a new peak appeared at 2θ: 42.140° corresponding to the (3 2 -3) crystalline plane of the monoclinic phase of $Bi_4O_5I_2$ (ICDD #98-041-2590) [39,40].

Therefore, these results suggest the presence of a heterojunction made by BiOI and $Bi_4O_5I_2$ crystalline structures[39–41]. On the other hand, after 30 min of calcination (Bi-30), no peaks corresponding to the crystalline planes of BiOI were detected. Consequently, the diffraction peaks located at 2θ: 9.301°, 24.141°, 28.937°, 31.602°, 36.955°, 42.140°, 45.336, 49.003°, 54.873°, 59.322°, and 66. 011 were fully indexed to the (1 0 -1), (3 1 0), (4 1 -1), (4 0 2), (-4 0 4), (3 2 -3), (4 2 2), (0 0 6), (8 1 1), (8 2 -2), and (8 0 4) crystal planes of the monoclinic phase of $Bi_4O_5I_2$ (ICDD #98-041-2590). Additionally, the XRD peaks of Bi-30 aligned well with the described XRD peaks reported for other $Bi_4O_5I_2$ materials, which indicates its high purity [39,40].

In the case of the Bi-45 sample, there was the appearance of new peaks located at 2θ: 7.742, 10.893°, 13.314°, 23.901°, 28.097°, 28.746°, 28.746°, 31.28°, 33.001°, 33.487°, 36.152°, 46.144°, 47.723°, 49.22°, 53.913°, 56.161°, and 58. 115° which were indexed to

the (0 0 1), (2 0 2), (2 0 1), (0 0 3), (3 1 2), (3 1 2), (0 0 4), (2 0 4), (0 2 0), (1 1 4), (0 2 4), (2 2 4), (7 1 3), (3 1 6), (9 1 2), (5 1 6) planes of the orthorhombic crystalline phase of Bi_5O_7I (ICDD #040-0548). Similar to Bi-15 sample, these results reveal the possible formation of a heterojunction between $Bi_4O_5I_2$ and Bi_5O_7I. Finally, when the sample was calcined for 60 min (Bi-60), only the peak located at 2θ 28.82° of $Bi_4O_5I_2$ was observed and more diffraction peaks corresponding to the orthorhombic phase of Bi_5O_7I (ICDD #040-0548) appeared at 2θ: 40.856°, 46.39°, 50.917°, 56.621°, 58.117°, 61.465°, and 64. 872° characteristic of the (0 0 5), (6 0 4), (1 1 6), (10 0 0), (6 2 4), (3 1 7), and (0 0 8) crystalline planes of the orthorhombic phase of Bi_5O_7I (ICDD #040-0548). Hence, these results suggest that by increasing the calcination time at a constant temperature (410 °C), it is possible to obtain different crystalline phases of $Bi_xO_yI_z$. As was observed, along the calcination time occurs a transition as follows BiOI → BiOI/$Bi_4O_5I_2$ → $Bi_4O_5I_2$ → $Bi_4O_5I_2$/Bi_5O_7I → Bi_5O_7I. This can be attributed to iodine release due to the heat treatment [30,34,41]. In addition, XRD analysis reveals an increase in the sharpness of the peaks as calcination time progresses, suggesting increased crystallinity [42]. Specifically, at 15, 30, 45 and 60 minutes, more defined peaks gradually appear, indicating a more ordered structuring.

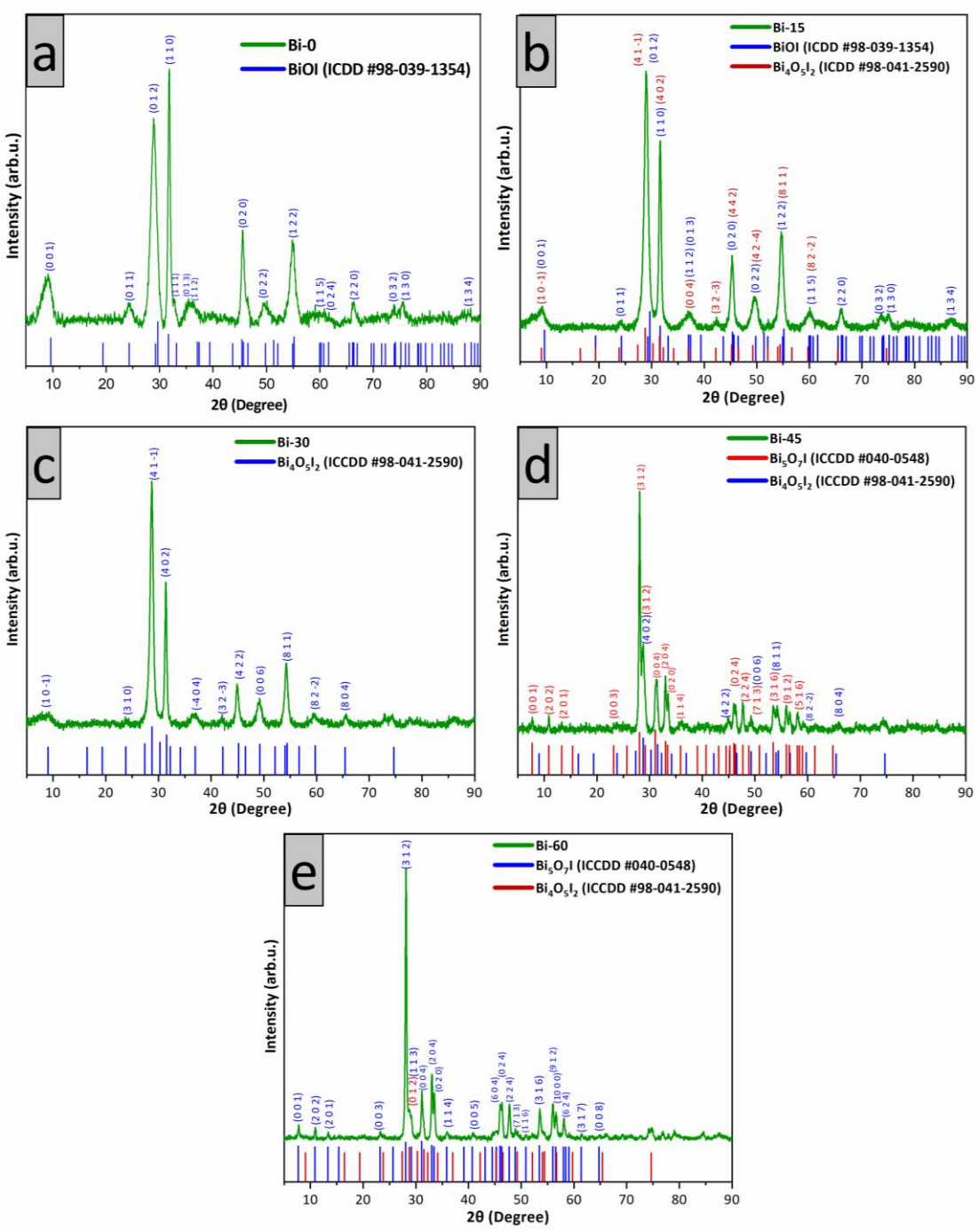

Figure. 1 XRD patterns of BiOI samples calcinated at different times: a) Bi-0, b) Bi-15, c) Bi-30, d) Bi-45, and e) Bi-60.

On the other hand, the crystallite sizes for samples Bi-0, Bi-15, Bi-30, Bi-45, and Bi-60 were determined to be 8.7, 9.07, 36.16, 18.1, and 24.34 nm, respectively. These results indicate a gradual increase of crystal size by increasing the calcination time from 0 to 45 min, and a subsequent decrease for the sample calcinated for 60 min. The increase of

the crystallite size from 0 to 30 min can be attributed to the thermal energy (410 °C) supplied to the material, which facilitates diffusion, and reorganization of the atoms into larger crystals [43]. In contrast, the subsequent decrease in Bi-45 and Bi-60 could be due to recrystallization [43] or collapse [19] of the crystal structure, due to the loss of higher iodine amount after 45 or 60 min than in 30 min [14,19,41]. Therefore, these results indicate that calcination time can alter the crystallite size of the material, which in turn can affects directly the photocatalytic activity.

3.1.2. Morphological and chemical characterization

The morphology of the photocatalysts obtained at different calcination times was analyzed by scanning electron microscopy. As is shown in Fig. 2a-b, the structures of the sample Bi-0 are flower-like microspheres assembled by well-defined and organized thin nanosheets. As is detailed in Table 1, these microspheres and the nanosheets stacked on their surface have an average diameter of 1.437 ± 0.016 and a thickness of 15.3 ± 0.447, respectively; However, after 15 min of annealing the thickness of the nanosheets increased (Table 1) resulting in a decrease of the total diameter of the microspheres (Table 1). In consequence, as seen in Fig. 2c-d, the ordering of the nanosheets undergo a slightly change. An additional increase in calcination time not caused a further decrease or increase of the diameter and thickness of the microspheres and nanosheets, respectively (Table 1).

However, as is observed in Fig 2e-j, the SEM images for B-30, B-45, and B-60 reveals a deformation of the nanosheets shape over the calcination time, resulting in microspheres with an irregular morphology after 60 min. This behavior can be attributed to the crystalline restructuring processes at long exposure times at elevated temperatures [43], as it was revealed by XRD, in which there was an increase in the crystallite size and a further decrease after 60 min of annealing. Therefore, these results underline the importance of controlling the calcination time to optimize the morphological and structural properties of materials for advanced applications such as photocatalysis.

Table 2. Evolution of the morphology of nanostructured flower-like microspheres: Diameter and thickness of $Bi_xO_yI_z$ as a function of time (0, 15, 30, 45 and 60 min) of calcination.

Samples	Time of calcination (min)	Microspheres Diameter (um)	Nanosheets thickness (nm)
B-0	0	1.437 ± 0.016	15.3 ± 0.447
B-15	15	1.192 ± 0.014	19.4 ± 0.390
B-30	30	1.140 ± 0.017	16.285 ± 0.409
B-45	45	1.088 ± 0.015	19.003 ± 1.509
B-60	60	1.144 ± 0.020	19.292 ± 0.501

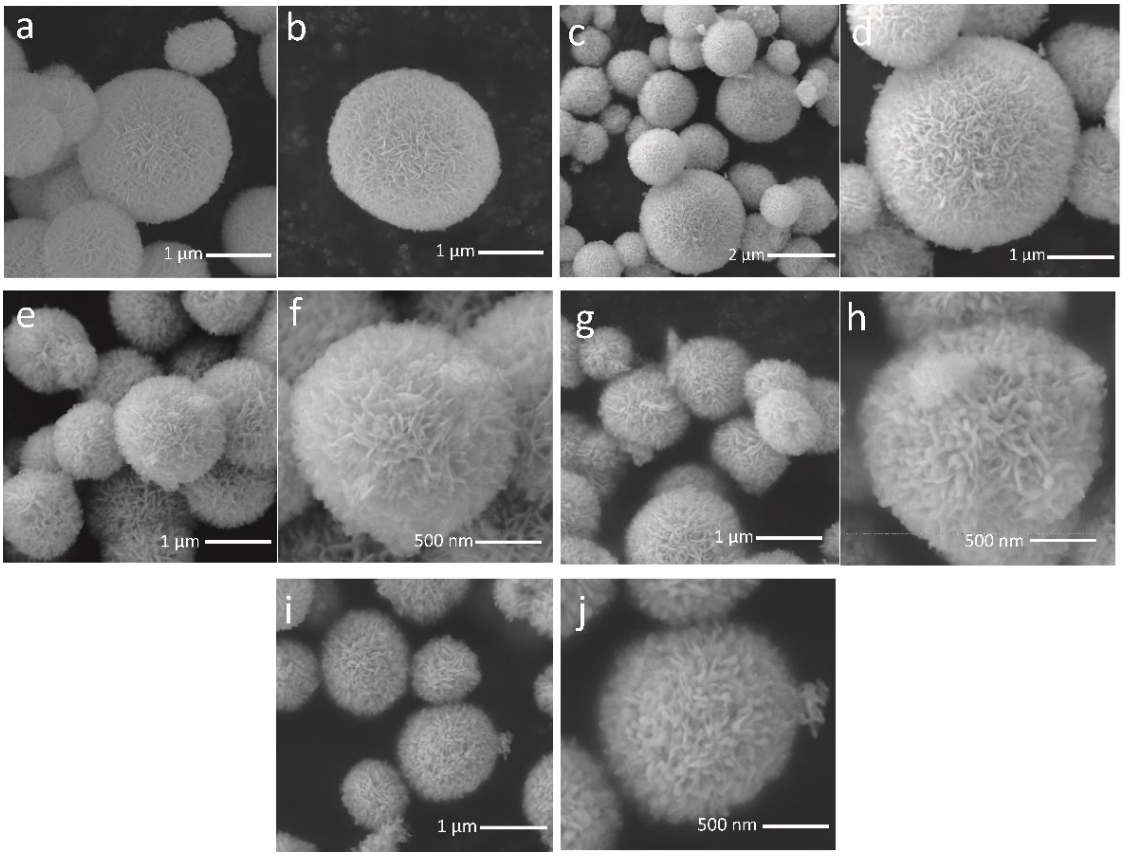

Figure. 2 SEM images of the samples synthesized at different calcination times Bi-0 (a-b), Bi-15 (c-d), Bi-30 (e-f), Bi-45 (g-h) and Bi-60 (i-j).

On the other hand, the chemical composition of the samples was determined by energy-dispersive X-ray spectroscopy. Fig. 3 confirmed the presence of bismuth (Bi), oxygen (O)

and iodine (I) in all calcinated samples. This was confirmed by elemental distribution maps presented in Fig. S1, which indicate a uniform and homogeneous distribution of Bi, O, and I in all the samples studied (Bi-0, Bi-15, Bi-30, Bi-45 and Bi-60). However, according to the inset Table in each figure, longer calcination time led to flower-like microspheres with a poor content of iodide and a higher concentration of Bi. These results are consistent with XRD analyses, in which there was a transition from BiOI crystalline phase to bismuth-rich bismuth oxyiodide crystalline phases due to iodine release induced by the thermal treatment. The increase of bismuth and loss of iodide could potentially broaden the band gap by causing a shift of the bottom and top position of the conduction and valence bands toward more negative and positive potentials, respectively [44]. As result, the redox potentials of the material can also be improved, leading to a stronger photocatalytic activity [45,46]. Furthermore, the tables at Fig. 3a-c reveal an initial increase of oxygen content in the samples from Bi-0 to Bi-30, followed by a gradual decrease in B-45 and Bi-60 (Fig. 3c-d). The increase of oxygen can be attributed to iodine loss and the decrease to the generation of oxygen vacancies, which can act as traps of photogenerated electrons and holes. Therefore, this phenomenon in combination with a wider band gap can decrease the recombination rate of photogenerated electrons and holes, resulting in a higher production of reactive oxygen species and degradation of target pollutant [30,34,47]. However, it is crucial to consider that an excessive increase in calcination time could result in excessive iodine desorption, negatively affecting the photocatalytic performance of the material due to changes in their crystallinity, electronic and optic properties [19,30].

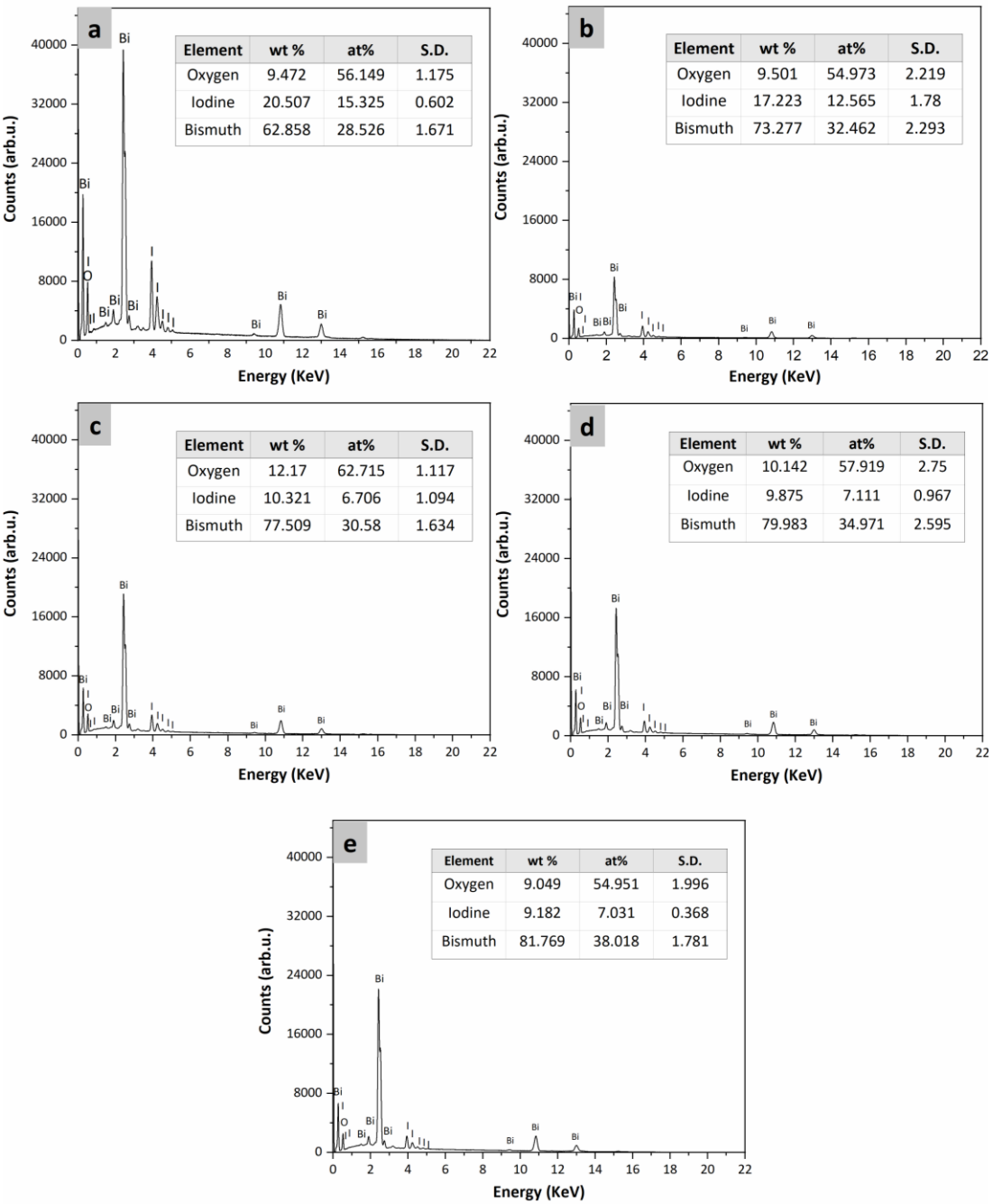

Figure. 3 Elemental analysis performed by EDS of samples synthesized and calcined at different times: (a) Bi-0, (b) Bi-15, (c) Bi-30, (d) Bi-45, and (e) Bi-60.

3.2. Photocatalytic degradation of Ibuprofen

The photocatalytic activity of the calcined microspheres was evaluated by the degradation of a 3 ppm solution of ibuprofen and the results are shown in Fig. 4. In Figure 4a, two main absorption bands were observed in the UV spectrum of the ibuprofen

solution: one at 192 nm, associated with the aggregation state of ibuprofen as a dimer in dilute aqueous solutions [48], and another at 222 nm, corresponding to the electronic π-π* transitions of the benzene ring [49]. Fig. 4b reveals no significant changes in the UV spectrum over the time under visible light irradiation, indicating that ibuprofen cannot be degraded directly by photons of the white LED light used in this work. However, Figure 4c-g shows a bathochromic shift from 222 nm to 226 nm after 60 min of darkness in the presence of the calcined samples. This shift is attributed to the deprotonation of ibuprofen due to pH changes induced by the semiconducting material [50], and the formation of intermediates with new functional groups or additional UV absorption groups (olefins, alcohols, ketones) due to the attack of reactive oxygen species (ROS) on ibuprofen [51]. Interestingly, the solution of ibuprofen exposed to BiOI showed a higher absorbance at 226 nm than the solution with the BiOI/$Bi_4O_5I_2$ heterojunction after 60 min in the dark (Figures 4c-d), which could indicate a higher adsorption capacity of the contaminant by the BiOI/$Bi_4O_5I_2$ heterostructure [52]. However, the behavior of absorbance changes at 226 nm and of new absorption bands after 60, 120 and 180 min suggests that these structures do not degrade ibuprofen. On the other hand, UV-vis spectra of ibuprofen exposed to Bi-30, Bi-45 and Bi-60 samples (Figures 4e-g) showed a new absorbance band at 262 nm after 60 min of visible light irradiation, possibly associated with p-Isobutylphenol, a by-product of ibuprofen degradation through hydroxylation, decarboxylation and demethylation processes induced by ROS attack [51,53–55]. Therefore, these results reveal the superior photocatalytic activity of Bi-30 ($Bi_4O_5I_2$), Bi-45 ($Bi_4O_5I_2$/Bi_5O_7I) and Bi-60 (Bi_5O_7I) in comparison with Bi-0 (BiOI) and Bi-15 (BiOI/$Bi_4O_5I_2$) [30,56].

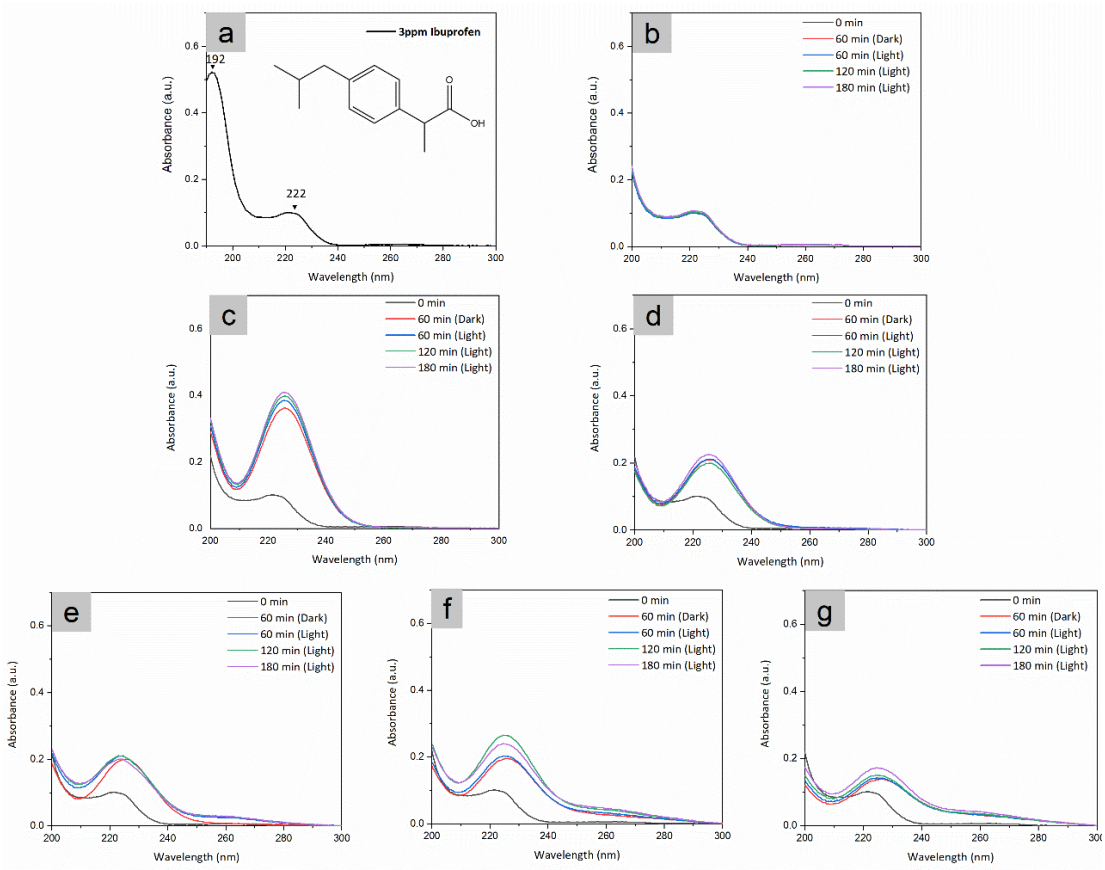

Figure. 4 UV–vis absorption spectra of samples: (a) 3 ppm ibuprofen (b) photolysis test of 3 ppm ibuprofen and photocatalytic degradation of ibuprofen using (c) B-0, (d) B-15, (e) B-30, (f) B-45, and (g) B-60.

The analysis of absorbance at 262 nm as a function of time, presented in Fig. 5, shows the efficacy of the photocatalysts Bi-30, Bi-45 and Bi-60 in the degradation of ibuprofen. While all three materials initially show an increase in absorbance, indicating the formation of by-products, sample Bi-30 exhibits a distinct behavior after 180 min of irradiation. After this point, a decrease in absorbance is observed, suggesting degradation of ibuprofen intermediates [55]. This observation points to the fact that Bi-30 exhibits a higher performance in the degradation of ibuprofen compared to Bi-45 and Bi-60. Therefore, sample Bi-30 is proposed as the photocatalyst with higher performance compared to the other semiconducting materials. This superior performance can be attributed to its larger crystallite size and possible enhancement of the redox potentials of the redox potentials of the individual BixOyIz materials. These characteristics decrease the rate of electron-hole pair recombination and favor the efficient generation of ROS, capable of degrading pollutants such as ibuprofen [19,30].

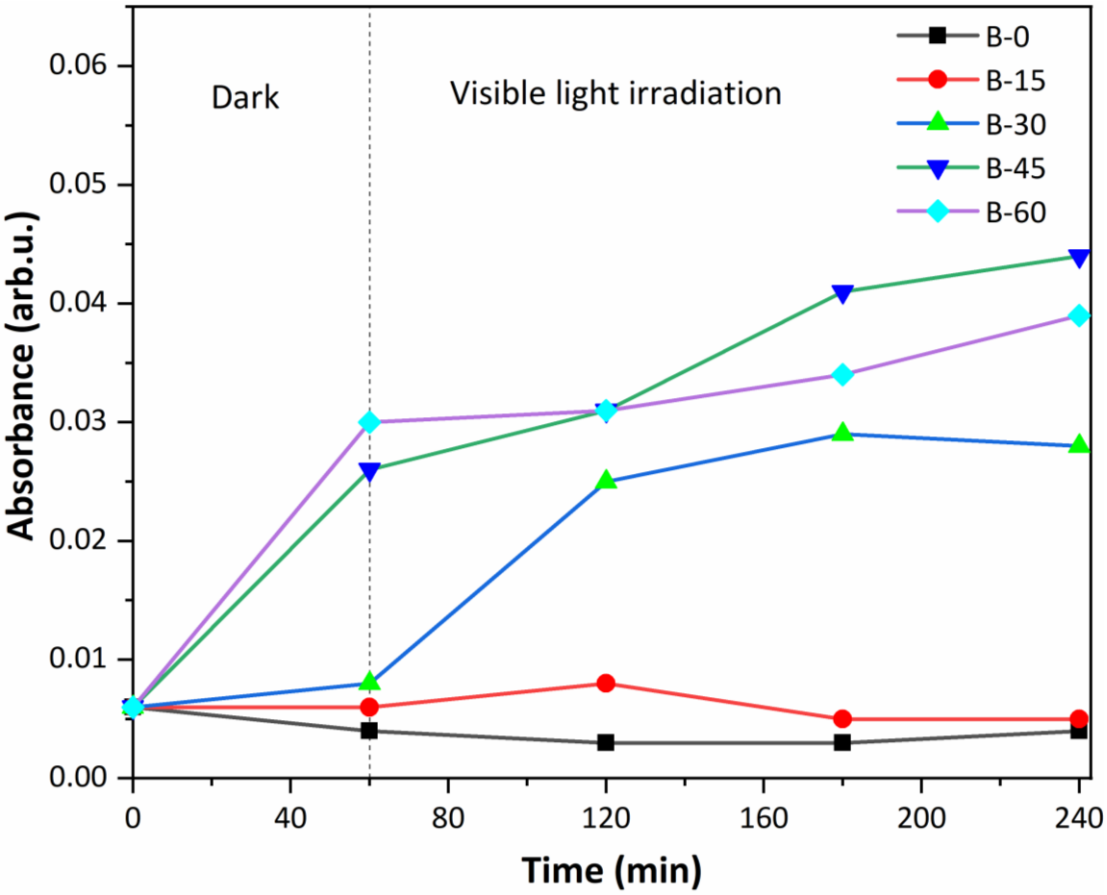

Figure. 5. Analysis of the absorbance at 262 nm for samples B-0, B-15, B-30, B-45 and B-60.

4. CONCLUSIONS

In this study, flower-shaped BixOyIz (BiOI, BiOI/ $Bi_4O_5I_2$, $Bi_4O_5I_2$, $Bi_4O_5I_2/Bi_5O_7I$) microspheres were successfully synthesized using a solvothermal method, followed by calcination at 410°C for 0, 15, 30, 45, and 60 min. Samples Bi-30, Bi-45 and Bi-60 exhibited higher photocatalytic performance in the degradation of ibuprofen compared to Bi-0 and Bi-15. However, Bi-30 demonstrated a superior ability than Bi-45 and Bi-60 to degrade ibuprofen intermediates after 180 min of irradiation. This higher efficiency is attributed to its larger crystallite size and improved redox potentials of the individual BixOyIz crystalline phases, which in turn favors a more efficient generation of reactive oxygen species. According to these results, it can be stated that adequate calcination time plays a fundamental role in shaping the structural, redox, and photocatalytic properties of BixOyIz microspheres. While excessive times can lead to iodine desorption and unfavorable morphological changes, which could negatively affect the material performance. Nonetheless, this work presents an optimal calcination time to obtain BixOyIz microspheres with improved properties, which in turn can be a potential candidate to be used in remediation of water bodies contaminated with Ibuprofen.

5. FUNDING SOURCES

This research was funded by Erasmus + CBHE consortium “Nature–based living lab for interdisciplinary practical and research semester on sustainable development and environmental protection in the amazon rainforest (Contract Number: 619346–EPP–1–2020–1–DE –EPPKA2–CBHE–JP).

6. AUTHOR CONTRIBUTIONS: CREDIT

Maria Auquilla-Villamagua: Conceptualization, Data curation, Methodology, Investigation, Writing – original draft. **Leonardo Proaño-Rhon:** Conceptualization, Data curation, Methodology, Investigation. **Michael Zuarez-Chamba:** Conceptualization, Methodology, Investigation, Writing – review & editing. **Karla Vizuete:** Investigation, Writing – review & editing. **Alexis Debut:** Investigation, Writing – review & editing. **Miguel Quishpe:** Supervision, Funding acquisition, Writing – review & editing. **Miguel Herrera-Robledo:** Supervision, Funding acquisition, Writing – review & editing.

7. ACKNOWLEDGMENT

Thanks to CENCINAT of the Universidad de las Fuerzas Armadas ESPE for the characterization of my semiconductor samples. Also, thanks to Eng. Andrea Salgado, and Eng. Carolina Ñacato for the support of working space and materials.

8. REFERENCES

1. Jan-Roblero J, Cruz-Maya Ja. Ibuprofen: Toxicology And Biodegradation Of An Emerging Contaminant. Molecules. 2023;28: 2097. Doi:10.3390/Molecules28052097
2. Chopra S, Kumar D. Ibuprofen As An Emerging Organic Contaminant In Environment, Distribution And Remediation. Heliyon. 2020;6. Doi:10.1016/J.Heliyon.2020.E04087
3. Parolini M, Binelli A, Provini A. Chronic Effects Induced By Ibuprofen On The Freshwater Bivalve Dreissena Polymorpha. Ecotoxicology And Environmental Safety. 2011;74: 1586–1594. Doi:10.1016/J.Ecoenv.2011.04.025
4. World Health Organization. Who Model Lists Of Essential Medicines. 2023 [Cited 23 Mar 2024]. Available: Https://Www.Who.Int/Groups/Expert-Committee-On-Selection-And-Use-Of-Essential-Medicines/Essential-Medicines-Lists
5. Brillas E. A Critical Review On Ibuprofen Removal From Synthetic Waters, Natural Waters, And Real Wastewaters By Advanced Oxidation Processes. Chemosphere. 2022;286: 131849. Doi:10.1016/J.Chemosphere.2021.131849
6. Osman Ai, Ayati A, Farghali M, Krivoshapkin P, Tanhaei B, Karimi-Maleh H, Et Al. Advanced Adsorbents For Ibuprofen Removal From Aquatic Environments: A Review. Environ Chem Lett. 2024;22: 373–418. Doi:10.1007/S10311-023-01647-6
7. Aus Der Beek T, Weber F-A, Bergmann A, Hickmann S, Ebert I, Hein A, Et Al. Pharmaceuticals In The Environment—Global Occurrences And Perspectives. Environmental Toxicology And Chemistry. 2016;35: 823–835. Doi:10.1002/Etc.3339
8. Rainsford K. Ibuprofen: Pharmacology, Efficacy And Safety | Inflammopharmacology. [Cited 3 Jun 2024]. Available: Https://Link.Springer.Com/Article/10.1007/S10787-009-0016-X
9. Liu J, Huang L, Li Y, Yang L, Wang C, Liu J, Et Al. Fabrication Oxygen Defect-Mediated Double Z-Scheme Bioi/Bio2−X/Biobr Photocatalyst For Pollutions Degradation And Bacteria Inactivation. Journal Of Environmental Chemical Engineering. 2022;10: 106668. Doi:10.1016/J.Jece.2021.106668
10. Chang C-J, Chen Y-C, Tsai Z-T. Effect Of Calcination Induced Phase Transition On The Photocatalytic Hydrogen Production Activity Of Bioi And Bi5o7i Based Photocatalysts. International Journal Of Hydrogen Energy. 2022;47: 40777–40786. Doi:10.1016/J.Ijhydene.2021.09.158
11. Han Q. Advances In Preparation Methods Of Bismuth-Based Photocatalysts. Chemical Engineering Journal. 2021;414: 127877. Doi:10.1016/J.Cej.2020.127877
12. Öchsner A, Da Silva Lfm, Altenbach H. Advanced Structured Materials. Springer. 2017 [Cited 6 Apr 2024]. Available: Https://Www.Springer.Com/Series/8611
13. Malefane Me, Feleni U, Mafa Pj, Kuvarega At. Fabrication Of Direct Z-Scheme Co3o4/Bioi For Ibuprofen And Trimethoprim Degradation Under Visible Light Irradiation. Applied Surface Science. 2020;514: 145940. Doi:10.1016/J.Apsusc.2020.145940

14. Ghali S, Mammeri L, Boucheloukh H, Sehili T. Controlled Solvothermal Synthesis Of Bi5o7i Nanoparticles For Enhanced Photocatalytic Degradation Of Paracetamol. Journal Of Photochemistry And Photobiology A: Chemistry. 2024;446: 115121. Doi:10.1016/J.Jphotochem.2023.115121
15. Hu Q, Dong J, Chen Y, Yi J, Xia J, Yin S, Et Al. In-Situ Construction Of Bifunctional Mil-125(Ti)/Bioi Reactive Adsorbent/Photocatalyst With Enhanced Removal Efficiency Of Organic Contaminants. Applied Surface Science. 2022;583: 152423. Doi:10.1016/J.Apsusc.2022.152423
16. Shu S, Wang H, Li Y, Liu J, Liu J, Yao J, Et Al. Fabrication Of N-P B-Bi2o3@Bioi Core/Shell Photocatalytic Heterostructure For The Removal Of Bacteria And Bisphenol A Under Led Light. Colloids And Surfaces B: Biointerfaces. 2023;221: 112957. Doi:10.1016/J.Colsurfb.2022.112957
17. Zhou H, Wu B, Dekanovsky L, Wei S, Khezri B, Hartman T, Et Al. Integration Of Bioi Nanosheets Into Bubble-Propelled Micromotors For Efficient Water Purification. Flatchem. 2021;30: 100294. Doi:10.1016/J.Flatc.2021.100294
18. Cheng H, Huang B, Dai Y. Engineering Biox (X = Cl, Br, I) Nanostructures For Highly Efficient Photocatalytic Applications. Nanoscale. 2014;6: 2009–2026. Doi:10.1039/C3nr05529a
19. Guan Y, Wu J, Man X, Liu Q, Qi Y, He P, Et Al. Rational Fabrication Of Flower-Like Bioi1-X Photocatalyst By Modulating Efficient Iodine Vacancies For Mercury Removal And Dft Study. Chemical Engineering Journal. 2020;396: 125234. Doi:10.1016/J.Cej.2020.125234
20. Xie Y-L, Guo L-F, Ben C-J. Fabrication Of Bioi Nanoflowers Decorated Tio2 Nanotube Arrays On Porous Titanium With Enhanced Photocatalytic Performance For Rhodamine B Degradation. International Journal Of Electrochemical Science. 2022;17: 22022. Doi:10.20964/2022.02.04
21. Long Y, Wang Y, Zhang D, Ju P, Sun Y. Facile Synthesis Of Bioi In Hierarchical Nanostructure Preparation And Its Photocatalytic Application To Organic Dye Removal And Biocidal Effect Of Bacteria. Journal Of Colloid And Interface Science. 2016;481: 47–56. Doi:10.1016/J.Jcis.2016.07.041
22. Hu C, Huang H-X, Lin Y-F, Yoshida M, Chen T-H. Decoration Of Srtio3 Nanofibers By Bioi For Photocatalytic Methyl Orange Degradation Under Visible Light Irradiation. Journal Of The Taiwan Institute Of Chemical Engineers. 2019;96: 264–272. Doi:10.1016/J.Jtice.2018.11.020
23. Kohantorabi M, Moussavi G, Oulego P, Giannakis S. Radical-Based Degradation Of Sulfamethoxazole Via Uva/Pms-Assisted Photocatalysis, Driven By Magnetically Separable Fe3o4@Ceo2@Bioi Nanospheres. Separation And Purification Technology. 2021;267: 118665. Doi:10.1016/J.Seppur.2021.118665
24. Hao R, Xiao X, Zuo X, Nan J, Zhang W. Efficient Adsorption And Visible-Light Photocatalytic Degradation Of Tetracycline Hydrochloride Using Mesoporous Bioi Microspheres. Journal Of Hazardous Materials. 2012;209–210: 137–145. Doi:10.1016/J.Jhazmat.2012.01.006
25. Zuarez-Chamba M, Tuba-Guamán D, Quishpe M, Vizuete K, Debut A, Herrera-Robledo M. Photocatalytic Degradation Of Bisphenol A On Bioi Nanostructured Films Under Visible Led Light Irradiation. Journal Of Photochemistry And Photobiology A: Chemistry. 2022;431: 114021. Doi:10.1016/J.Jphotochem.2022.114021

26. Di J, Xia J, Ji M, Wang B, Yin S, Xu H, Et Al. Carbon Quantum Dots Induced Ultrasmall Bioi Nanosheets With Assembled Hollow Structures For Broad Spectrum Photocatalytic Activity And Mechanism Insight. Langmuir. 2016;32: 2075–2084. Doi:10.1021/Acs.Langmuir.5b04308
27. Zhang A, Xing W, Zhang D, Wang H, Chen G, Xiang J. A Novel Low-Cost Method For Hg0 Removal From Flue Gas By Visible-Light-Driven Biox (X = Cl, Br, I) Photocatalysts. Catalysis Communications. 2016;87: 57–61. Doi:10.1016/J.Catcom.2016.09.003
28. Ma S, Li Y, Luo X, Zhao S, Cao Z, Ding Y, Et Al. Dislocation-Rich Bioi Nanosheets Designed By Nitrogen Ion Implantation For Improving Nir-Triggered Bactericidal Activity. Materials Today Energy. 2023;31: 101214. Doi:10.1016/J.Mtener.2022.101214
29. Yu J, Wang B. Effect Of Calcination Temperature On Morphology And Photoelectrochemical Properties Of Anodized Titanium Dioxide Nanotube Arrays. Applied Catalysis B: Environmental. 2010;94: 295–302. Doi:10.1016/J.Apcatb.2009.12.003
30. Matiur Rm, Abuelwafa Aa, Putri Aa, Kato S, Kishi N, Soga T. Annealing Effects On Structural And Photovoltaic Properties Of The Dip-Silar-Prepared Bismuth Oxyhalides (Bioi, Bi7o9i3, Bi5o7i) Films. Sn Appl Sci. 2021;3: 138. Doi:10.1007/S42452-021-04153-Y
31. Zhang Q, Gao L, Guo J. Effects Of Calcination On The Photocatalytic Properties Of Nanosized Tio2 Powders Prepared By Ticl4 Hydrolysis. Applied Catalysis B: Environmental. 2000;26: 207–215. Doi:10.1016/S0926-3373(00)00122-3
32. Chang A-M, Chen Y-H, Lai C-C, Pu Y-C. Synergistic Effects Of Surface Passivation And Charge Separation To Improve Photo-Electrochemical Performance Of Bioi Nanoflakes By Au Nanoparticle Decoration. Acs Appl Mater Interfaces. 2021;13: 5721–5730. Doi:10.1021/Acsami.0c18430
33. Fu S, Li G, Wen X, Fan C, Liu J, Zhang X, Et Al. Effect Of Calcination Temperature On Microstructure And Photocatalytic Activity Of Biox (X=Cl, Br). Transactions Of Nonferrous Metals Society Of China. 2020;30: 765–773. Doi:10.1016/S1003-6326(20)65252-9
34. Putri Aa, Kato S, Kishi N, Soga T. Study Of Annealing Temperature Effect On The Photovoltaic Performance Of Bioi-Based Materials. Applied Sciences. 2019;9: 3342. Doi:10.3390/App9163342
35. Huang H, Xiao K, Zhang T, Dong F, Zhang Y. Rational Design On 3d Hierarchical Bismuth Oxyiodides Via In Situ Self-Template Phase Transformation And Phase-Junction Construction For Optimizing Photocatalysis Against Diverse Contaminants. Applied Catalysis B: Environmental. 2017;203: 879–888. Doi:10.1016/J.Apcatb.2016.10.082
36. Min Gu Kim, Jeong Min Kang, Ji Eun Lee, Kang Seok Kim, Kwang Ho Kim, Min Cho, Et Al. Effects Of Calcination Temperature On The Phase Composition, Photocatalytic Degradation, And Virucidal Activities Of Tio2 Nanoparticles. [Cited 21 Jun 2024]. Available: Https://Pubs.Acs.Org/Doi/10.1021/Acsomega.1c00043
37. Park Jy, Ae Yang Seo, Chae Hee Park, Jun Hyung Lim, Jinho Joo. Effects Of Calcination Temperature On Morphology, Microstructure, And Photocatalytic Performance Of Tio2 Mesocrystals. [Cited 21 Jun 2024]. Available: Https://Pubs.Acs.Org/Doi/10.1021/Acs.Iecr.7b01920

38. Usman Ak, Aris A, Labaran Ba, Darwish M, Jagaba Ah. Effect Of Calcination Temperature On The Morphology, Crystallinity, And Photocatalytic Activity Of Zno/Tio2 In Selenite Photoreduction From Aqueous Phase. [Cited 21 Jun 2024]. Doi:10.14447/Jnmes.V25i4.A05
39. Cheng H, Wu J, Tian F, Zhao L, Ji Z, Li F, Et Al. In-Situ Crystallization For Fabrication Of Bioi/Bi4o5i2 Heterojunction For Enhanced Visible-Light Photocatalytic Performance. Materials Letters. 2018;232: 191–195. Doi:10.1016/J.Matlet.2018.08.119
40. Xiao X, Lin Y, Pan B, Fan W, Huang Y. Photocatalytic Degradation Of Methyl Orange By Bioi/Bi4o5i2 Microspheres Under Visible Light Irradiation. Inorganic Chemistry Communications. 2018;93: 65–68. Doi:10.1016/J.Inoche.2018.05.009
41. Zichen Shen, Huanzhen Liu, Xuemei Jia, Qiaofeng Han, Huiping Bi. Phase Transformation And Heterojunction Construction Of Bismuth Oxyiodides By Grinding-Assisted Calcination In The Presence Of Thiourea And Their Photoactivity - Dalton Transactions (Rsc Publishing). [Cited 14 Jun 2024]. Available: Https://Pubs.Rsc.Org/En/Content/Articlelanding/2021/Dt/D1dt00745a/Unauth
42. Liu J, Li H, Du N, Song S, Hou W. Synthesis, Characterization, And Visible-Light Photocatalytic Activity Of Bioi Hierarchical Flower-Like Microspheres. Rsc Adv. 2014;4: 31393–31399. Doi:10.1039/C4ra04829f
43. Ashraf R, Riaz S, Kayani Zn, Naseem S. Effect Of Calcination On Properties Of Zno Nanoparticles. Materials Today: Proceedings. 2015;2: 5468–5472. Doi:10.1016/J.Matpr.2015.11.071
44. Jin X, Ye L, Xie H, Chen G. Bismuth-Rich Bismuth Oxyhalides For Environmental And Energy Photocatalysis. Coordination Chemistry Reviews. 2017;349: 84–101. Doi:10.1016/J.Ccr.2017.08.010
45. Chen X, Shen W, Liang D, Quhe R, Wang S, Guan P, Et Al. Effects Of Bi On Band Gap Bowing In Inp1-Xbix Alloys. Opt Mater Express, Ome. 2018;8: 1184–1192. Doi:10.1364/Ome.8.001184
46. Newnham J, Zhao T, Quin Dg, Manning| Td, Zanella Marco E, Daniels L, Et Al. And Structure Engineering Of Bi4o4secl2 For Thermoelectric Applications. [Cited 15 Jun 2024]. Available: Https://Pubs.Acs.Org/Doi/10.1021/Acsorginorgau.2c00018
47. Ji M, Chen R, Di J, Liu Y, Li K, Chen Z, Et Al. Oxygen Vacancies Modulated Bi-Rich Bismuth Oxyiodide Microspheres With Tunable Valence Band Position To Boost The Photocatalytic Activity. Journal Of Colloid And Interface Science. 2019;533: 612–620. Doi:10.1016/J.Jcis.2018.08.097
48. Marbán G, Fernández-Pérez A, Álvarez-García S. Ultraviolet Light Spectroscopic Characterization Of Ibuprofen Acid Aggregation In Deionized Water. Heliyon. 2023;9: E21260. Doi:10.1016/J.Heliyon.2023.E21260
49. Brahmi C, Benltifa M, Ghali M, Dumur F, Simonnet-Jégat C, Valérie M, Et Al. Performance Improvement Of The Photocatalytic Process For The Degradation Of Pharmaceutical Compounds Using New Pom/Polymer Photocatalysts. Journal Of Environmental Chemical Engineering. 2021;9: 106015. Doi:10.1016/J.Jece.2021.106015
50. Padilla Villavicencio M, Escobedo Morales A, Ruiz Peralta Ma De L, Sánchez-Cantú M, Rojas Blanco L, Chigo Anota E, Et Al. Ibuprofen Photodegradation By Ag2o And Ag/Ag2o Composites Under Simulated Visible Light Irradiation. Catal Lett. 2020;150: 2385–2399. Doi:10.1007/S10562-020-03139-6

51. Tian H, Fan Y, Zhao Y, Liu L. Elimination Of Ibuprofen And Its Relative Photo-Induced Toxicity By Mesoporous Biobr Under Simulated Solar Light Irradiation. Rsc Adv. 2014;4: 13061. Doi:10.1039/C3ra47304j

52. Bai J, Sun J, Zhu X, Liu J, Zhang H, Yin X-B, Et Al. Enhancement Of Solar-Driven Photocatalytic Activity Of Bioi Nanosheets Through Predominant Exposed High Energy Facets And Vacancy Engineering. Small. 2020;16: 1904783. Doi:10.1002/Smll.201904783

53. Maicon Oliveira Miranda, Wesley Euĺ Alio Cabral Cavalcanti, Felipe Fernandes Barbosa, Joś E Antonio De Sousa, Francisco Ivan Da Silva, Tiago Pinheiro Braga. Photocatalytic Degradation Of Ibuprofen Using Titanium Oxide: Insights Into The Mechanism And Preferential Attack Of Radicals - Rsc Advances (Rsc Publishing). [Cited 25 Jun 2024]. Available: Https://Pubs.Rsc.Org/En/Content/Articlehtml/2021/Ra/D1ra04340d

54. Arthur Rb, Bonin Jl, Ardill Lp, Rourk Ej, Patterson Hh, Stemmler Ea. Photocatalytic Degradation Of Ibuprofen Over Biocl Nanosheets With Identification Of Intermediates. Journal Of Hazardous Materials. 2018;358: 1–9. Doi:10.1016/J.Jhazmat.2018.06.018

55. Photocatalytic Degradation Of Non-Steroidal Anti-Inflammatory Drugs With Tio2 And Simulated Solar Irradiation - Sciencedirect. [Cited 5 Jul 2024]. Available: Https://Www.Sciencedirect.Com/Science/Article/Abs/Pii/S0043135407005313

56. Tu S, Lu M, Xiao X, Zheng C, Zhong H, Zuo X, Et Al. Flower-Like Bi 4 O 5 I 2 /Bi 5 O 7 I Nanocomposite: Facile Hydrothermal Synthesis And Efficient Photocatalytic Degradation Of Propylparaben Under Visible-Light Irradiation. Rsc Adv. 2016;6: 44552–44560. Doi:10.1039/C6ra03988j

9. SUPPLEMENTARY MATERIAL

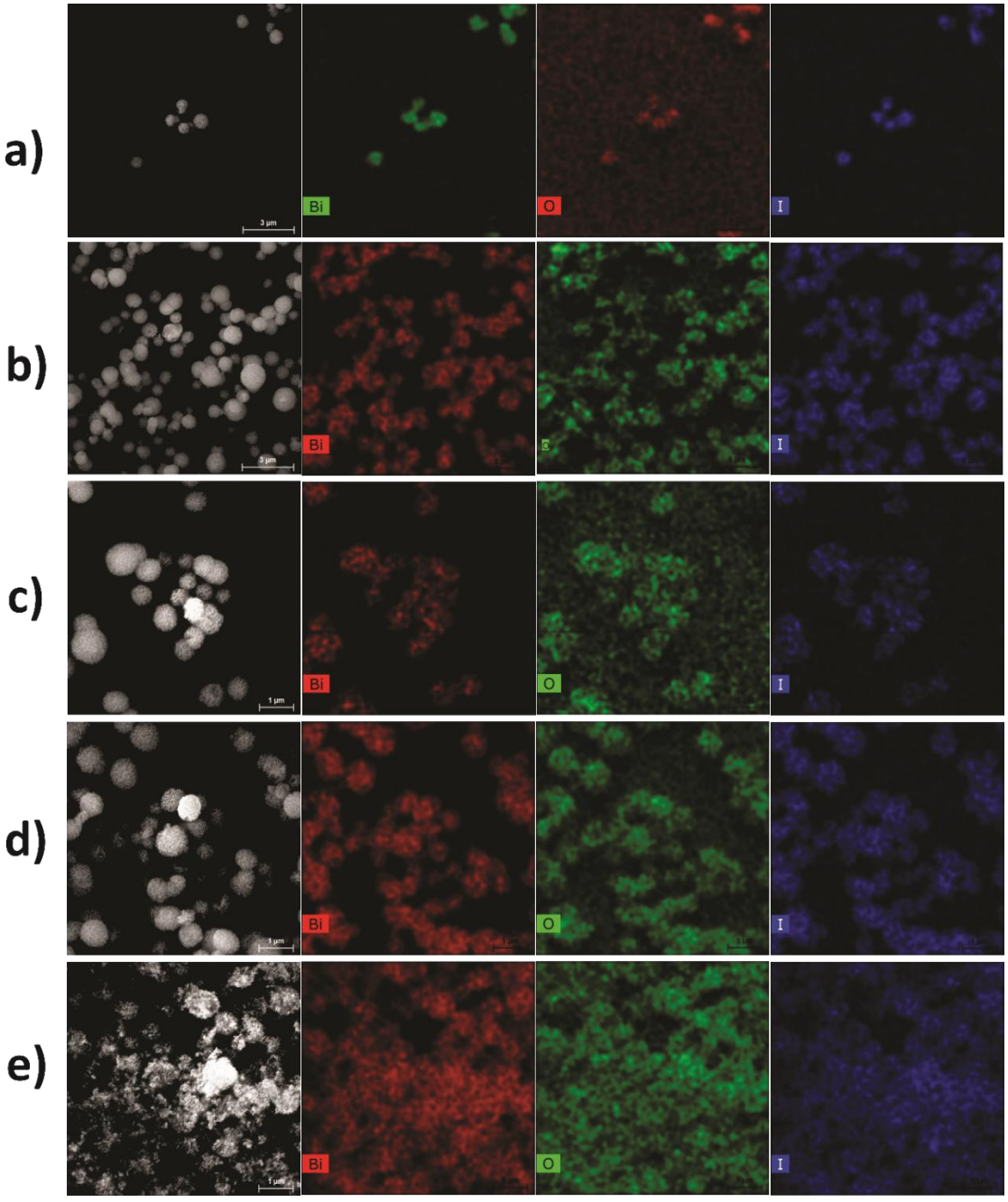

Figure S 1. Mapping of sample: (a) Bi-0, (b) Bi-15, (c) Bi-30, (d) Bi-45, and (e) Bi-60.